SAND2020-6293C

Uncertainty Quantification of Leading Edge Erosion Impacts on Wind Turbine Performance

David C. Maniaci[1], Carsten Westergaard[1], Alan Hsieh[1], and Joshua A. Paquette[1]

[1]Sandia National Laboratories, Albuquerque, NM 87185
Corresponding author: dcmania@sandia.gov

Keywords: Leading Edge Erosion, Uncertainty Quantification

Abstract. Many factors that influence the effect of leading edge erosion on annual energy production are uncertain, such as the time to initiation, damage growth rate, the blade design, operational conditions, and atmospheric conditions. In this work, we explore how the uncertain parameters that drive leading edge erosion impact wind turbine power performance using a combination of uncertainty quantification and wind turbine modelling tools, at both low and medium fidelity. Results will include the predicted effect of erosion on several example wind plant sites for representative ranges of wind turbine designs, with a goal of helping wind plant operators better decide mitigation strategies.

1. Introduction

Leading edge erosion (LEE) is a prominent issue in wind turbine blade reliability, causing gradual performance decreases and persistent maintenance costs. It is generally understood that the main driver of erosion is the impact of rain droplets on the leading edge. The erosion rate is a function of the joint probability of rainfall frequency, droplet size, wind speed, rotor speed, blade skin construction, and other parameters. The repeat impact on the blade skin does not initially cause any damage until a certain threshold is reached. Once this incubation period has elapsed, the leading-edge erosion generally makes the leading edge a bit rough, similar to a dirty or pitted surface. The initial damage category is commonly labeled 1 or 2 and generally considered cosmetic in its nature. The aerodynamic impact of such conditions have been studied elaborately in numerous wind tunnel studies [1-12], and the annual energy loss can be quantified using such data. The AEP loss is up to 2% for this light level of erosion. Such losses are generally, very difficult to detect in ordinary power curve measurements or production numbers, so these types of damages are generally not repaired.

As the repeat rain drop impact penetrates the outer coating, minor structural damage occurs as the underlying fiber glass matrix is gradually exposed. These damages start as category 3 damage and transition into category 4. Depending on the repair priorities, these two categories generally result in repair efforts based on visual inspections. An example of a category 4 damage is shown in figure 1, from which an imprint was tested in the wind tunnel [9,12]. The AEP impact is significant, but also not easily detectable in a measured power curve, especially considering that the degradation occurs over many years. Results of an in-depth study indicated that a heavily eroded wind turbine blade can reduce annual energy production by up to 5% for a utility scale wind turbine based on the NREL 5-MW turbine model,

see [7]. Ultimately, the damage reaches a category 5, where the hollow of the blade is exposed and severe structural damage becomes eminent and the turbine must be stopped and repaired urgently.

Figure 1. Category 4 damage from which an imprint reproduction of the eroded leading edge was tested in the wind tunnel [9, 12].

2. Industry-level Analysis

In order to illustrate the importance of leading-edge erosion across a broad fleet, the USGS wind turbine database was used [13], including only turbines in larger wind farms constructed after year 2000. The fleet of 48,536 turbines in 925 wind farms is made up almost of 100 different turbine models and a total capacity of 92 GW. The database does not include RPM data, so this input has been manually entered for the 100 turbine models from their data sheets. For simplicity, it is assumed that all turbines within each state experience the state average rain rate. The average annual windspeed is scaled with the hub height relative to 7.5 m/s and 80m of each turbine with a wind shear exponent of 0.14, $U_{avg} = 7.5 \cdot (hh \,/\, 80)^{0.14}$. These data sources and assumptions result in raw capacity factors ranging from 36 to 47%. During the period shown in figure 2, the average rotor diameter has increased steadily from 70 to 119 meters; whereas, the average turbine tip speed remained in the 76-78 m/s range until 2010, after which new turbines have significantly increased in tip speed.

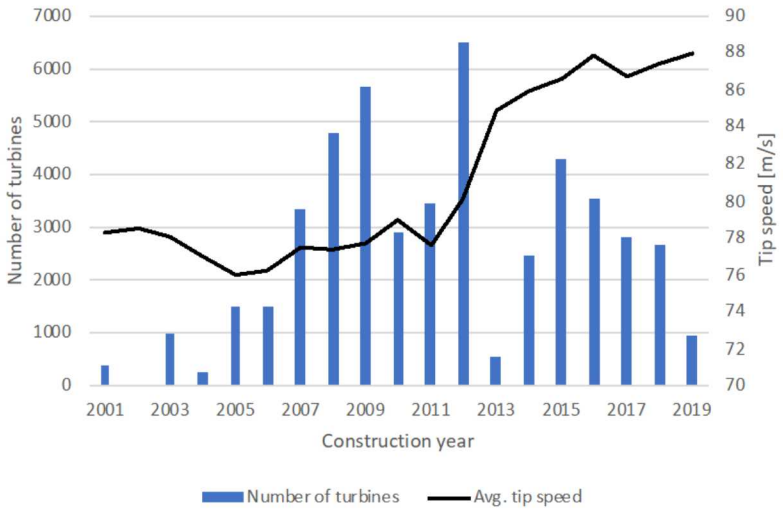

Figure 2. Number of turbines constructed and the average US fleetwide tip speed extracted from [13], supplemented with RPM information.

The predominant driver of leading-edge erosion is the local speed of rain drops relative to the blade speed, so in part driven by the terminal velocity of the drops and in part by the turbine rotational speed. The rate of erosion is suggested to be proportional to $V^{6.7}$, where V is the local velocity as defined in [14] and proportional to the rain rate or volume of rain to the power of 2/3. Using this sensitivity to erosion rates, we can compute the relative erosion rate with reference to the year 2000's average tip velocity. This illustrates an increased risk of erosion by a factor 2.5 over the period considered, see figure 3. Obviously, this is under the assumption that no turbine leading edge has been reinforced or equipped with leading edge protection.

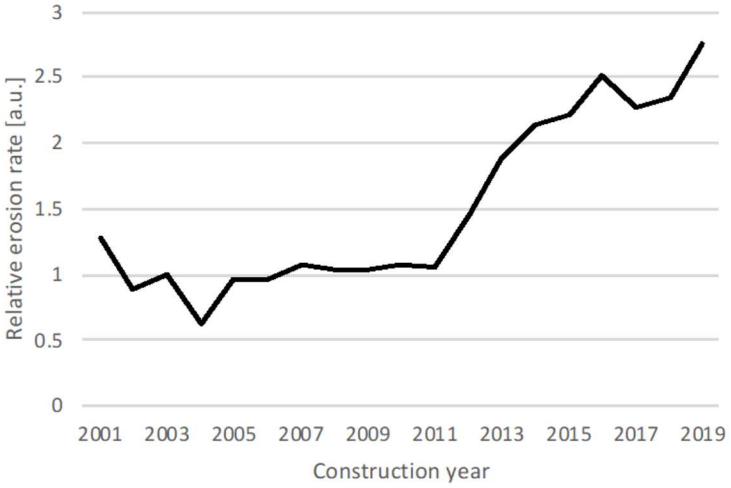

Figure 3. Average erosion rate of the US fleet newer than year 2000, computed based on tip velocity and state-wide average rain rate using the sensitivity suggested in [14].

The turbine suppliers and leading-edge protection (LEP) suppliers have in recent years adapted the ASTM G73-10 whirling arm rain erosion test, where blade sections are tested with an accelerated rate of speeds up to 160 m/s, rain rates up to 35 mm/hour and droplets sizes between 1 to 2 mm. In principle, this can be correlated to the real-life turbine experience with tip speeds between 80 to 110 m/s, rain rates up to 4500 mm/year and droplets exceeding the test droplet diameter [15,16]. While velocity and rain intensity are relatively easily translated between test and experiment, the sensitivity to droplet size is more difficult to quantify because of the lack of site-specific droplet information combined with actual turbine operational speeds. The sensitivity to droplet size is high; and, it has been suggested [15] that rather than implementing LEP to reduce rain impact, the turbine can be de-rated with a reduced tip speed during events when the rain drop distribution include large droplets. Both methods are likely to reduce annual energy production up to a few percentage points.

Since we do not have an accurate translation between the tested resilience and the real world LE durability, we can explore a more pragmatic approach to derive erosion impact on the US fleet. Firstly, it would be reasonable to assume that the time to reach the point of repair is inversely proportional to the relative erosion rate. Further, based on the experience that older turbines generally need repair after 10 to 15 years of operation, we can compute how many turbines in the fleet need repair relative to their construction year using the theoretical growth rate computed for each individual turbine in each individual wind farm. Regardless of the accuracy of these simple assumptions, figure 4 illustrates the increased interest in LEE for the US fleet. If the trigger point for repair is significant LEE detected by visual inspection, the associated annual energy losses are significant and increasing. The number of repairs tapers off because future turbine construction is unknown and thus not added. One could speculate, that perhaps new leading-edge systems or operational modifications could also reduce the future efforts on LE repairs.

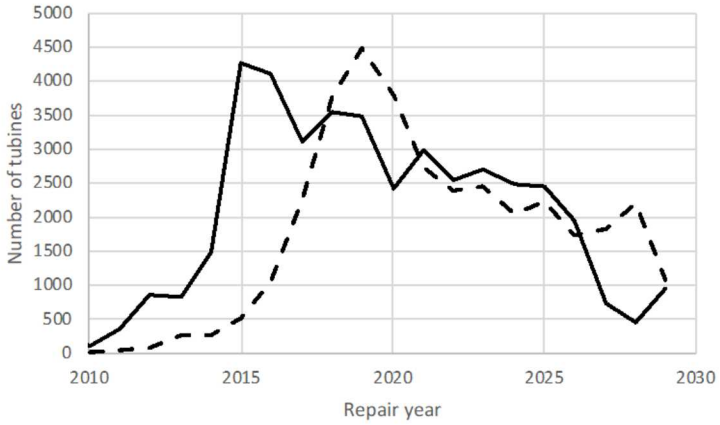

Figure 4. Number of turbines in the existing US fleet needing LEE repair, assuming 10 (solid) to 15 years (dash) offset time to repair, scaled with the relative erosion rate described in figure 3.

Another risk aspect of new turbines entering the market is simply that new turbines with larger rotor diameters, generally have a higher capacity factor [17] and therefore spend more operating hours at full rated RPM and tip-speed. In figure 5, we have shown an older US turbine compared to a newer class III turbine, compared with U_{avg}=7.5 m/s wind Rayleigh distribution. The difference in rated wind speed is 1.0 m/s. While that may not seem like much, the new turbine will spend 710 hours more per year at rate power than the older one. Everything else even, this increases the risk of the turbine being at a high tip speed though rain weather, thus increase the amount of leading-edge erosion. However, while the rate of erosion may be higher, the effect on performance is mitigated to some extent, as more time is spent in region III vs. region II operation.

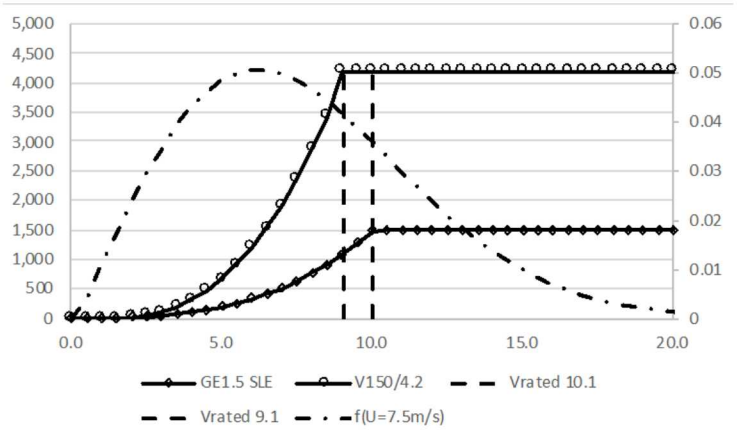

Figure 5. Power curves of a typical turbine constructed in year 2004 to 2011 and an example of a new high capacity factor IEC class III new turbine, which has not entered the market yet, shown with a Rayleigh distribution U_{avg}=7.5m/s.

Understanding the range of impact of erosion on performance will help wind plant operators decide when to mitigate the effects of this erosion through repairs, modifications, or changes in operation. Some of the assumptions of the preceding high-level analysis include the effect of erosion on airfoil performance, the effect of the spanwise distribution of erosion on turbine power, and the influence of the turbine controller on the performance of an eroded turbine. In the remainder of this work, these parameters will be estimated in greater detail for several categories of blade erosion and their impact on performance will be explored using a standard static power curve and a probabilistic power curve cloud analysis.

3. Detailed Analysis - Power Curve Uncertainty

As previously discussed, erosion is dependent on a variety of weather and turbine design parameters. While there remains much research to do in producing validated, physics-based models of erosion, there are already a number of coating solutions available. Thus, a current uncertainty that exists in industry is the economics, specifically in how and when to repair blades and the extent to which de-rating should be employed. This will be of larger concern in the future as blade designs will likely be lighter and operate at higher tip speeds, while markets will move from power-purchase agreements to merchant operation, incentivizing plant owners to better understand real-time performance and costs.

To more thoroughly understand one part of this problem, a probabilistic analysis of the impact on aerodynamic power performance from leading edge erosion was undertaken. The main focus of this analysis is to estimate the AEP loss that can be expected from erosion from a realistic power curve, which feeds into the high-level analysis used to make operational decisions to mitigate erosion through control or repair. This analysis will also serve to predict the level of erosion that can be detected within the limits of power curve uncertainty.

There are several important components to predicting loss in power and AEP from leading edge erosion for a given erosion level. The first is creating a map from the rate of erosion at each spanwise station to the tested erosion of the wind turbine blades' airfoils. A method was also created to estimate how the erosion progresses along the span of the wind turbine blade as the erosion level increases. These methods were then used to generate simulated eroded blades, whose power loss was modelled using a standard static power curve analysis. A probabilistic analysis was then undertaken to produce a power curve cloud, simulating the uncertainty in measuring changes to a power curve on an operational wind turbine.

3.1. Eroded Airfoil Performance Modeling

Modeling the impacts of erosion on power in more detail for a specific turbine requires detailed clean and eroded airfoil polar (lift and drag) data, as well as details of the complete turbine design and control system. For the example analysis in the present study, the National Rotor Testbed (NRT) turbine was selected, as its design information is publicly available and field test data will be as well [18]. Further, the NRT rotors were designed to reproduce the wake and performance characteristics of 2000's era utility wind turbines, and thus currently represent some of the most prevalent in operation today.

The rotor blades use two primary airfoils along the blade span: the 24% thick S814 airfoil on the inner part of the blade and the 17% thick S825 airfoil on the outer part [18]. These airfoils were designed as part of a family for a variable speed, pitch regulated turbine, and include more modern wind turbine airfoil design considerations such as roughness insensitivity and high lift coefficient design [19]. The S825 airfoil is used along the outer half of the NRT blades, and has been tested under clean, transition fixed, and standard roughness conditions at the NASA Low Turbulence Pressure Tunnel [19]. The clean S825 airfoil wind tunnel data from the NASA tests were used in this study.

Erosion starts near the blade tip at regions of the highest impact velocity and progresses inboard. Simulating eroded blades only requires the airfoil polar data for the eroded surface conditions in the outer blade sections to be modified. Unfortunately, detailed eroded experimental data is not available for the S825 airfoil; however, data is available from previous work for a similar airfoil, the NACA 63_3-418, which is also widely used in the industry for this generation of turbines.

During the wind tunnel testing at Texas A&M, the NACA 63_3-418 airfoil was tested with a range of roughness levels and a reproduction of severe erosion from an operational wind turbine [1,3,5]. The results from severe erosion were termed the eroded leading edge (ELE) and are equivalent to the higher erosion level considered in the performance analysis in this paper (category 4), see figure 1. The ELE results from Texas A&M show drag lower than fixed transition for low lift, but much higher than fixed transition at higher lift where wind turbines operate in Region 2 operation. Since the eroded leading edge shows unique performance characteristics not tested on the S825 airfoil, the modified performance characteristics of this NACA airfoil were applied to the clean S825 wind tunnel data as an offset in drag and lift coefficients for a given zero-lift corrected angle of attack, as shown in figure 6. This simple

method was deemed appropriate since the clean drag polars of these airfoils are similar in the design conditions of a wind turbine blade (lift coefficient ~1.0-1.2). Additionally, this modified ELE polar is bounded by the NASA S825 wind tunnel data transition fixed and standard roughness test cases until higher lift is reached, where it shows higher drag than even the rough test conditions. The effect of category 1-3 levels of erosion on the S825 airfoil were then estimated from linear interpolation between the clean airfoil polar and the category 4 ELE polar.

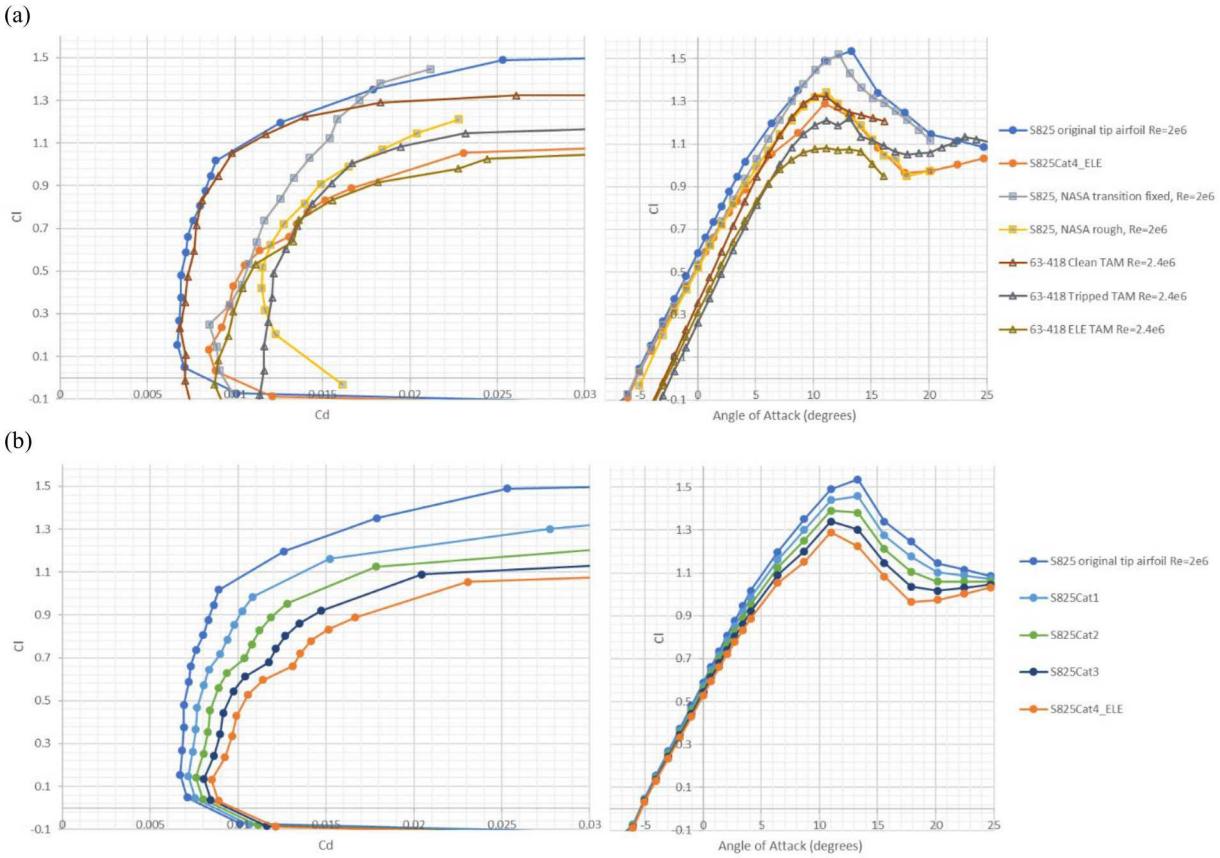

Figure 6. (a) Lift and drag polars from NASA wind tunnel tests of the S825 airfoil and of the NACA 63_3-418 airfoil from Texas A&M. (b) Modified S825 eroded airfoil polars based on the eroded leading edge wind tunnel tests at Texas A&M of the NACA 63_3-418 airfoil.

3.2. Blade Erosion Modeling

Leading edge erosion is caused primarily by fatigue induced by the impact of rain or hail on the leading edge surface material, making it a strong function of the impact velocity that is in turn a function of the tip speed and spanwise location along the blade. Erosion is most severe near the blade tip, and decreases toward blade mid-span. The erosion rate was made proportional to the incoming velocity on a blade section to an exponent of 6.7 [14]. This estimate ignores the effect of the reduction in particle impacts near the airfoil surface due to stagnation and flow around the airfoil surface, which would act to reduce the impact velocity [2,9]. In this work we have chosen not to include such secondary effects and rely on the 6.7 exponent to represent all accumulated effects. Categories of blade erosion were defined by the airfoil erosion category over the outer 5% of the blade. The erosion level then declines inboard based on the impact velocity exponent, resulting in the blade spanwise erosion distributions in figure 7.

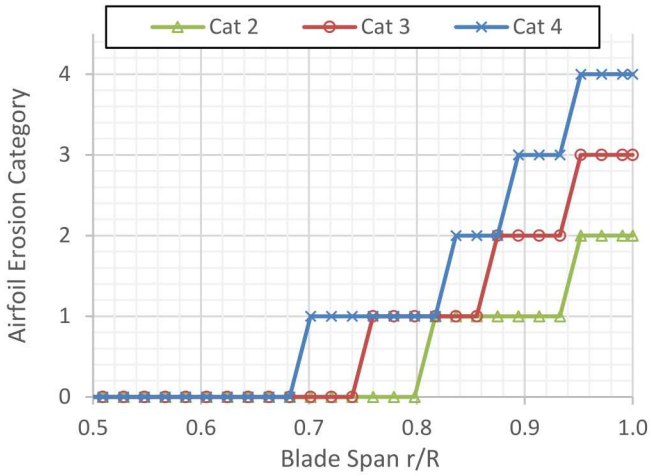

Figure 7. Spanwise location of erosion along each blade for three categories of blade erosion. The blade categories correspond to the level of airfoil section erosion on the outer 5% of the blade and progress inboard based on the computed local erosion rate.

For a steady state analysis, the power curve of the NRT turbine was computed using the clean and three eroded blade models in the OpenFAST code suite with the AeroDYN subroutine and uniform wind inflow [20]. The mean generator power of thirty second simulations were used in 1 m/s increments from 3 m/s to 14 m/s to construct the power curve in figure 8; 0.25 m/s increments were used between 11 m/s and 14 m/s for higher resolution of the region right before rated power. It was assumed that the power is the same during region III operation regardless of erosion level. As the erosion level increases, power production decreases and the transition to rated power operation becomes more gradual. The power relative to the non-eroded blade is shown in figure 9, with category 4 erosion producing approximately a 3% loss in power prior to rated power.

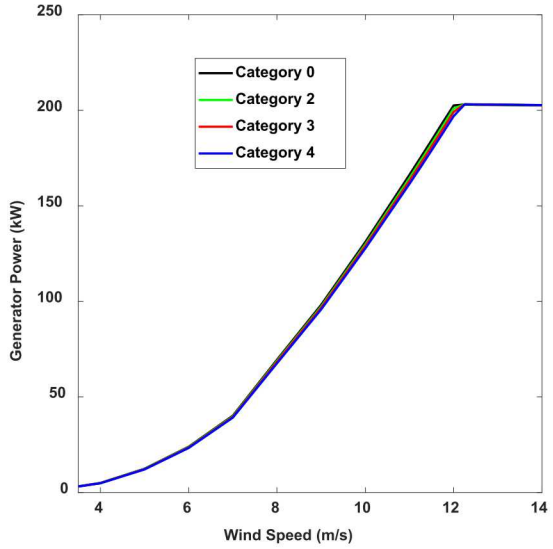

Figure 8. Steady power curve for the different levels of erosion using a steady state analysis.

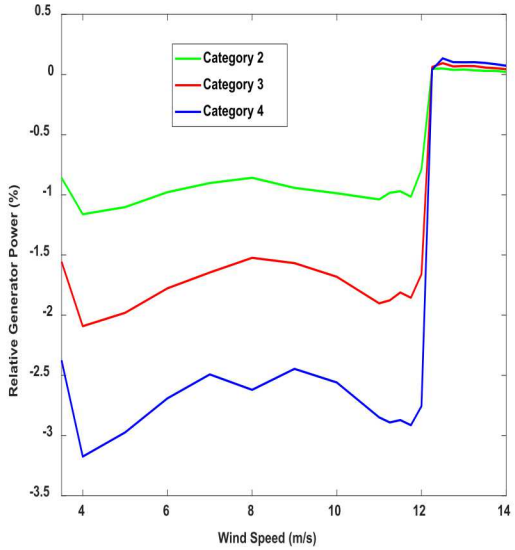

Figure 9. Difference in steady power curves for the three erosion levels.

3.3. Power Curve Uncertainty Analysis Method

For the dynamic forward propagation uncertainty quantification (UQ) study, TurbSim [21] was used to generate the unsteady atmospheric inflow and the OpenFAST code suite was used to model the coupled dynamic response of the NRT turbine. Monte Carlo sampling was conducted to randomly sample 10,000 simulations, each 10 minutes long, for each of the four erosion categories using six uncertain aleatoric parameters: hub-height wind speed, turbulence intensity (TI), the vertical power-law wind-shear exponent, air density, turbine yaw offset and collective blade pitch. The samples were taken from normal distributions of the aforementioned parameters with the respective means and standard deviations shown in Table 1. These values in Table 1 were informed by experimental data from the wake steering experiment at the Sandia Scaled Wind Farm Technology (SWiFT) site [22]. The TurbSim and OpenFAST simulations were scheduled and run using Dakota [23], an uncertainty quantification toolkit developed by Sandia National Laboratories which provides a flexible interface between the simulation codes and sampling-based uncertainty quantification. Dakota also provides parallel computing capabilities, which allows for hundreds of independent simulations to be run concurrently on Sandia's high-performance capacity cluster systems.

Table 1: Summary of uncertain aleatoric parameters in the dynamic UQ study. derived from the real operating conditions at the SWiFT site [20].

Parameter	Units	Mean	St. Dev.
Hub-Height Wind Speed	[m s^{-1}]	8.69	1.6673
Turbulence intensity	[%]	10.80	6.50
Shear exponent	[-]	0.14	0.1713
Air Density	[kg m^{-3}]	1.02	0.0281
Yaw Offset	[deg]	0.00	7.9950
Collective Blade Pitch	[deg]	1.00	0.0483

The results of the probabilistic eroded power curve study are shown in figures 10 and 11. The power curve clouds in figure 10 do not show a clear difference between the erosion levels. But the relative generator power difference between the best fit of each power curve to that of the uneroded curve, shown in figure 11, shows distinct disparities between the eroded categories. At low wind speeds, the results for lower erosion levels (category 2 and 3) show an increase in power, but this trend is likely due to the combination of a lower number of samples away from the mean sampled wind speed and that the relative variance in power due to the random changes in the input parameters may be larger than the change in power due to erosion. If this study had been parametric, meaning that each of the eroded blade cases were simulated for the same 10,000 samples, then the increased relative power at low wind speeds for the category 2 and 3 erosion blades would likely disappear, but then this study would not simulate the uncertainty of testing turbines in the field. The small number of random samples at the low wind speeds are not sufficient to reduce the variance due to the inflow parameters below that of the effect of erosion. Also, this indicates that power reduction due to erosion may be difficult to detect from field measurements at low wind speeds as the uncertainties associated with the atmospheric inflow and turbine operation are more significant than erosion effects. At moderate wind speeds, which are more important for total energy production, more samples were taken due to the normal distribution for wind speed. The difference in power for moderate wind speeds is more similar to the steady power curve results shown in figure 8. In the middle of region II the power difference appears marginal, but near rated power the influence of erosion gradually becomes clearer in the power curve. After rated wind speed, the power curves were assumed to converge, although this assumption will be explored in future work.

Table 2 contains the difference in annual energy production (AEP) relative to the clean, non-eroded blade for three categories of blade erosion and four mean wind speeds using a Rayleigh probability distribution of wind speed. The lowest 4 m/s mean wind speed case is not a standard wind class and

was included to illustrate the effect of erosion with minimal region III operation, where power is regulated based on generator and turbine load limits. The results show that as the mean wind speed increases, the impact of erosion on AEP decreases due to longer relative operation in region III above rated wind speed. These results indicate that the difference in power production due to leading edge erosion should be distinguishable between turbines that are similarly calibrated in the field given enough sampling time.

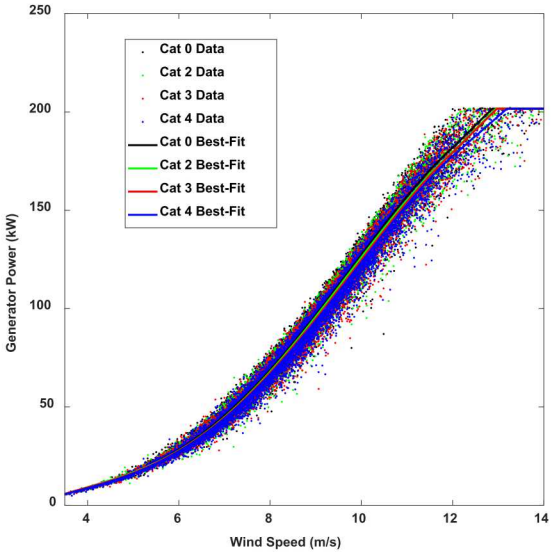

Figure 10. Power curve cloud generated with the probabilistic uncertainty quantification method. Best fit curves of each power curve cloud are also included.

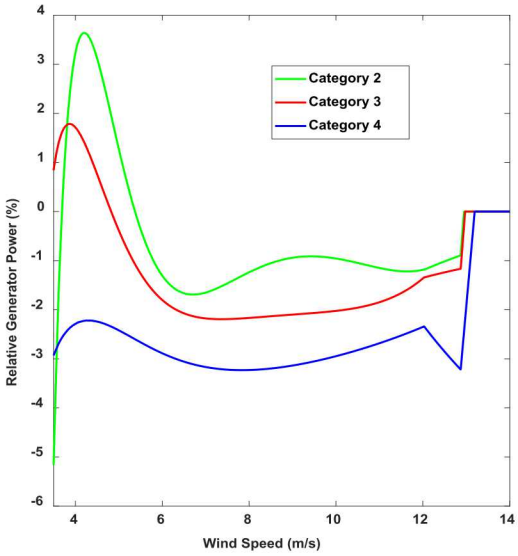

Figure 11. Difference in power between the best fit power curves for the three erosion levels.

Table 2. Annual energy production relative to no erosion for a range of mean wind speeds using a Rayleigh wind distribution, based on the power curve cloud results.

	Mean Wind Speed (m/s)				
Erosion Category	4	6	7.5	8.5	10
0	0.0%	0.0%	0.0%	0.0%	0.0%
2	-1.0%	-0.9%	-0.7%	-0.6%	-0.4%
3	-1.9%	-1.6%	-1.3%	-1.1%	-0.8%
4	-3.0%	-2.6%	-2.2%	-1.9%	-1.6%

4. Conclusion

This paper summarized a high level analysis of the issue of erosion for the US wind turbine fleet, and then performed a more detailed analysis on the difference in power curves between different blade erosion levels. These sources of uncertainty were estimated based on past work and propagated to the impact to annual energy production using the uncertainty quantification tool Dakota that ran instances of the wind turbine modeling tool OpenFAST. Future work will keep expanding this detailed analysis to include more parameters, such as erosion rate due to droplet size and frequency distributions, different control and maintenance strategies, uncertainty in airfoil performance, and different turbine designs.

This article was prepared by Sandia National Laboratories (SNL) Albuquerque, NM, 87185, U.S.A. SNL is a multi-mission laboratory managed and operated by National Technology and Engineering Solutions of Sandia, LLC., a wholly owned subsidiary of Honeywell International, Inc., for the U.S. Department of Energy's National Nuclear Security Administration under contract DE-NA-0003525. Funding was provided by the U.S. Department of Energy's Wind Energy Technologies Office.

5. References

[1] Ehrmann, R.S., et al., *Realistic Leading-Edge Roughness Effects on Airfoil Performance*, in *31st AIAA Applied Aerodynamics Conference*. 2013, American Institute of Aeronautics and Astronautics.

[2] Wilcox, B. and E. White, *Computational analysis of insect impingement patterns on wind turbine blades. Wind Energy*, 2016. 19(3): p. 483-495.

[3] Ehrmann, R.S., et al., *Effect of Surface Roughness on Wind Turbine Performance*. 2017, Sandia National Laboratories: Albuquerque, NM. p. 114. SAND2017-10669.

[4] Langel, C.M., et al., *A Computational Approach to Simulating the Effects of Realistic Surface Roughness on Boundary Layer Transition*, in 52nd Aerospace Sciences Meeting. 2014, American Institute of Aeronautics and Astronautics.

[5] Ehrmann, R.S. and E.B. White, *Influence of 2D Steps and Distributed Roughness on Transition on a NACA 63(3)-418*, in 32nd ASME Wind Energy Symposium. 2014, American Institute of Aeronautics and Astronautics.

[6] Langel, C.M., et al., *A Transport Equation Approach to Modeling the Influence of Surface Roughness on Boundary Layer Transition*. 2017, Sandia National Laboratories: Albuquerque, NM. p. 100. SAND2017-10670.

[7] Langel, C.M., et al., *Analysis of the Impact of Leading Edge Surface Degradation on Wind Turbine Performance,* in 33rd Wind Energy Symposium. 2015, American Institute of Aeronautics and Astronautics.

[8] Langel, C.M., R. Chow, and C.P. VanDam, *Further Developments to a Local Correlation Based Roughness Model for Boundary Layer Transition Prediction*, in 53rd AIAA Aerospace Sciences Meeting. 2015, American Institute of Aeronautics and Astronautics.

[9] Maniaci, David Charles, Ed White, Benjamin Wilcox, Christopher Langel, Case Van Dam, and Paquette, Joshua. *Experimental Measurement and CFD Model Development of Thick Wind Turbine Airfoils with Leading Edge Erosion*. United States: N. p., 2017. Web. doi:10.1088/1742-6596/753/2/022013.

[10] Maniaci, D.C., et al., *Experimental Measurement and CFD Model Development of Thick Wind Turbine Airfoils with Leading Edge Erosion*. Journal of Physics: Conference Series, 2016. 753(2): p. 022013.

[11] Wilcox, B., E.B. White, and D.C. Maniaci, *Roughness Sensitivity Comparisons of Wind Turbine Blade Sections*. 2017, Sandia National Laboratories: Albuquerque, NM. p. 118. SAND2017-11288.

[12] Ehrmann, Robert S., and White, E. B. *Effect of Blade Roughness on Transition and Wind Turbine Performance.*. United States: N. p., 2015. *Preprint, Web.* https://www.osti.gov/servlets/purl/1427238.

[13] Hoen, B.D., Diffendorfer, J.E., Rand, J.T., Kramer, L.A., Garrity, C.P., Hunt, H.E. (2020) United States *Wind Turbine Database*. U.S. Geological Survey, American Wind Energy Association, and Lawrence Berkeley National Laboratory data release: USWTDB V2.3 (January, 2020). https://eerscmap.usgs.gov/uswtdb.

[14] Eisenberg, D., Laustsen, S., Stege, J, *Leading Edge Protection Lifetime Prediction Model Creation and Validation*, Wind Europe, Hamburg, 27 to 29 September, 2016, PO.078g

[15] Bech, J. I., Hasager, C. B., & Bak, C. (2018). *Extending the life of wind turbine blade leading edges by reducing the tip speed during extreme precipitation events*. Wind Energy Science, 3(2), 729-748. https://doi.org/10.5194/wes-3-729-2018.

[16] Haag, M. D., *Secure annual energy production by a leap in leading edge protection of wind turbine blades*, Sandia Blade workshop 2014, Albuquerque, 2014.

[17] Wiser, Ryan H, and Bolinger, Mark. 2018 Wind Technologies Market Report. United States: N. p., 2019. Web. doi:10.2172/1559241.

[18] Kelley, Christopher Lee. *Aerodynamic design of the National Rotor Testbed*. 2015. SAND-2015-8989.

[19] Somers D M 2005 Design and Experimental Results for the S825 Airfoil. NREL/SR-500-36346.

[20] "NWTC Information Portal (OpenFAST)," ed. https://nwtc.nrel.gov/OpenFAST. Last modified 14-June-2016; Accessed 05-December-2019.

[21] "NWTC Information Portal (TurbSim)," ed. https://nwtc.nrel.gov/TurbSim. Last modified 5-Jan-2018; Accessed 04-December-2019.

[22] J. Berg et al., *Scaled Wind Farm Technology Facility Overview*, in AIAA SciTech 32nd Wind Energy Symposium, 2014.

[23] Adams, B.M., Bauman, L.E., Bohnho, W.J., Dalbey, K.R., Ebeida, M.S., Eddy, J.P., Eldred, M.S., Geraci, G., Hooper, R.W., Hough, P.D., Hu, K.T., Jakeman, J.D., Maupin, K.A., Monschke, J.A., Rushdi, A., Swiler, L.P., Vigil, D.M, and Wildey, T.M., *Dakota, A Multilevel Parallel Object-Oriented Framework for Design Optimization, Parameter Estimation, Uncertainty Quantification, and Sensitivity Analysis: Version 6.0 Users Manual*. Sandia National Laboratories SAND2014-4633. Updated November 2016 (Version 6.5).